Hindawi
Journal of Chemistry
Volume 2020, Article ID 4310513, 8 pages
https://doi.org/10.1155/2020/4310513

Research Article

Photocatalytic Degradation of Rhodamine B by C and N Codoped TiO_2 Nanoparticles under Visible-Light Irradiation

Thuy Thi Thanh Le[1] **and Trinh Dinh Tran**[2]

[1]*Department of Chemistry, Faculty of Science, Qui Nhon University, No. 170 an Duong Vuong Street, Qui Nhon, Vietnam*
[2]*VNU Key Laboratory of Advanced Materials for Green Growth, Faculty of Chemistry, University of Science, Vietnam National University, No. 334 Nguyen Trai Street, Hanoi, Vietnam*

Correspondence should be addressed to Thuy Thi Thanh Le; lethithanhthuy@qnu.edu.vn and Trinh Dinh Tran; trinhtd@vnu.edu.vn

Received 18 April 2020; Revised 6 June 2020; Accepted 18 June 2020; Published 9 July 2020

Guest Editor: Tapan Sarkar

C and N codoped TiO_2 nanoparticles were synthesized via a solvothermal method. The degradation of Rhodamine B by the photocatalyst C, N-TiO_2 was investigated under visible-light irradiation generated by using a 36 W compact fluorescent lamp which is characterized by wavelengths from 400 to 650 nm. The structure and properties of the obtained photocatalyst have been systematically investigated using X-ray diffraction, TEM, UV-Vis, FT-IR, and BET techniques. The experimental results revealed that C, N codoped TiO_2 nanoparticles were successfully synthesized, with an average diameter of 9.1 nm. C, N-TiO_2 nanoparticles exhibited an energy band gap of 2.90 eV, which were lower than pristine TiO_2 (3.34 eV), C-TiO_2 (3.2 eV), and N-TiO_2 (3.03 eV). The degradation of Rhodamine B by C, N-TiO_2 indicated that, under visible-light irradiation, the optimal dose of the photocatalyst was 1.8 g/L, and the removal of Rhodamine B was almost complete after 3 hours of reaction. The photocatalytic degradation of Rhodamine B in the range of 5–100 mg/L showed that the process followed the first-order kinetics according to the Langmuir–Hinshelwood model. The highest apparent rate constant (0.0427 min^{-1}) was obtained when the initial concentration of Rhodamine B was 5 mg/L, whereas the former decreased with the increase in the initial concentration of Rhodamine B. Moreover, C and N codoped TiO_2 nanoparticles presented a high potential for recycling, which was characterized by a removal efficiency of more than 86% after three cycles.

1. Introduction

TiO_2 is one of the well-known photocatalysts because of its nontoxicity, chemical stability, ease of processing, low cost, and multiple reusability. However, TiO_2 is only active under the ultraviolet light (Eg~3.2 eV in the anatase phase), which prevents it from various applications. The doping of nonmetals such as N, C, S, P, and halogens in TiO_2 would lead to an increase in catalytic activities in the visible-light region [1–5]. Particularly, the modification of TiO_2 by carbon increases the photosensitivity of the obtained materials [1, 2]. It has been reported that N-doping TiO_2 could result in a significant decrease in the energy band gap and an increase in catalytic activity in the visible-light region [3, 4].

Rhodamine B (RhB) has been widely used in histologic specimens; textile, paper, and cosmetics industries; RhB is also a well-known water tracer fluorescent [6]. RhB is harmful to humans and animals. Expose to RhB was reported to cause acute symptoms such as burning of the eyes, excessive tearing, nasal burning and itching, chest pain/tightness and burning, rhinorrhea, cough, burning of the throat, headache, and nausea [7]. The carcinogenicity and reproductive and developmental toxicity of RhB to humans and animals have been experimentally proven [8, 9]. Therefore, a number of efforts to remove RhB from the aqueous medium have been made. Several techniques have been deployed to deal with RhB residues in waters such as flotation [10, 11], activated sludge process [12], chemical

oxidation [13, 14], adsorption [15–17], and membrane filtration [18, 19]. Recently, advanced oxidation processes (AOPs) in a particular photocatalytic approach have been widely applied for the degradation of RhB in waters. For instance, Phuruangrat et al. [20, 21] studied parameters influencing RhB degradation in a solution by Bi_2WO_6-based catalysts and found that at optimal conditions, RhB degradation efficiency could reach more than 98%. Similarly, Lee et al. [22] reported that a photocatalyst based on a polydimethylsiloxane (PDMS)-TiO_2-gold (Au) composite was able to degrade about 85% of RhB after 90 min of visible-light irradiation. That photocatalytic system also presented a high potential of recyclability, with a degradation efficiency of more than 80% after four cycles of RhB treatment. Le et al. [23] revealed synergic effects in the Fe-C-TiO_2/AC photocatalytic system and reported a very good catalytic activity of the system for the degradation of RhB in solutions under visible-light irradiation. After five cycles, there were still more than 80% of RhB in solutions degraded by the Fe-C-TiO_2/AC photocatalytic system. Similar results were reported by previous studies [24, 25]. Until now, no work reports on the degradation of RhB by the C, N-TiO_2 photocatalyst.

In this work, C and N codoped TiO_2 was prepared by combination of the sol-gel and hydrothermal methods. The main objective is to shift light absorption from the UV region to the visible-light region apart from the increase in photocatalytic activity of as-synthesized photocatalysts. Different parameters influencing the photodegradation of RhB by C and N codoped TiO_2 photocatalysts were studied, while the photodegradation of C and N codoped TiO_2 was described by using the Langmuir–Hinshelwood equation.

2. Experimental

2.1. Catalyst Preparation. Chemicals: TIOT (tetraisopropyl orthotitanate 98%), nitric acid (HNO_3 68%), ethyl alcohol (C_2H_5OH 99.7%) and ammonium chloride (NH_4Cl) pure, and Rhodamine B ($C_{28}H_{31}ClN_2O_3$) were used. Synthesis of C, N-TiO_2: firstly, two solutions A and B were prepared separately. Solution A was obtained by well mixing 6 mL TIOT with 50 mL C_2H_5OH, while solution B contained a mixture of 28 mL C_2H_5OH, 0.4 mL HNO_3 (68%), 1.6 mL of distilled water, and 850 mg NH_4Cl. Solution A was dropped into the solution B under vigorous agitation at room temperature for 2 hours to form a uniform and transparent sol solution. Sol was then aged for 2 days at room temperature to form gel which was then placed into a Teflon-lined stainless steel autoclave and heated at 180°C for 10 hours. After the hydrothermal treatment, the obtained solid was washed using distilled water, prior to being dried at 100°C for 24 hours. The C, N-TiO_2 catalyst was collected after being pulverized in an agate mortar [26–28].

2.2. Photocatalytic Degradation Experiment. To investigate the optimal catalyst dosage, 100 mL RhB (20 mg/L) was firstly poured into a beaker (250 mL), which was then added with x (g/L) of the catalyst ($x = 1.4$, 1.8, 2.6, and 3.0 g/L). Then, the obtained solution was stirred with a constant speed for 30 min in the black light to reach the absorption equilibrium. Finally, the solution was irradiated by a 36 W compact fluorescent lamp, and the decomposition time was counted since then. The RhB concentration during the reaction was measured by the photometry method. The removal efficiency of the RhB bay photocatalyst (H%) is calculated based on the initial concentration of RhB (C_0) and concentration of RhB (C_t) at time (t), according to the following equation:

$$H(\%) = 100 \cdot \frac{(C_0 - C_t)}{C_0}. \quad (1)$$

The effect of irradiation conditions on the RhB decomposition was also investigated. The experiments were carried out in the dark, natural light at noon, and lights from a 36 W compact fluorescent lamp. The light characteristics of the deployed compact lamp were examined by using a PMS-50 spectrophotocolorimeter which showed that the deployed compact lamp emitted light in the region of 400–650 nm (Figure S1).

2.3. Characterization Techniques. Crystallite phases of the obtained materials were identified by X-ray diffraction (XRD) measurements (D8 Advance 5005). A scanning electron microscope (SEM, Hitachi S4800) and a transmission electron microscope (TEM, JEOL JEM-1010 electron microscope) have been used to investigate the particle size and morphology of the samples. Wavelength absorption was conducted by UV-Vis (Jasco-V670 photospectrometer). Elemental composition of the catalyst was determined by energy-dispersive X-ray spectroscopy, EDX (JEOL-JSM 6490). Functional groups were identified by IR spectroscopy (IR prestige 21). Nitrogen isothermal adsorption (Brunauer–Emmett–Teller (BET)) was done by TriStar 3000 V6.07 A. RhB concentrations were determined by UV-Vis at 553 nm (the absorption maximum wavelength of RhB).

3. Results and Discussion

3.1. Characterization of C and N Codoped TiO_2. As can be seen in Figure 1, unmodified TiO_2 exhibits the characteristic peaks of both anatase (A) and rutile (R) crystal phases, while modified TiO_2 only shows the characteristics peaks of the anatase crystal phase at 2θ of 25.26°; 37.78°; 38.56°; 48.00°; 53.90°; and 63.92°. This indicates that the C and N codoping in TiO_2 has an effect on the phase formation of the obtained material, which may be attributed to an increase in its catalytic activity [27]. The average crystallite size of C, N-TiO_2 calculated by using Scherrer's equation is 9.1 nm. This is in good agreement with the results of TEM (Figure 2) measurement. It is noted that the average crystallite size of C and N codoped TiO_2 is smaller than that of unmodified TiO_2.

The UV-Vis spectra of the prepared photocatalysts are presented in Figures 3 and 4. The results show that the absorption band of C and N codoping TiO_2 (C, N-TiO_2) was significantly expanded to the visible region compared to the

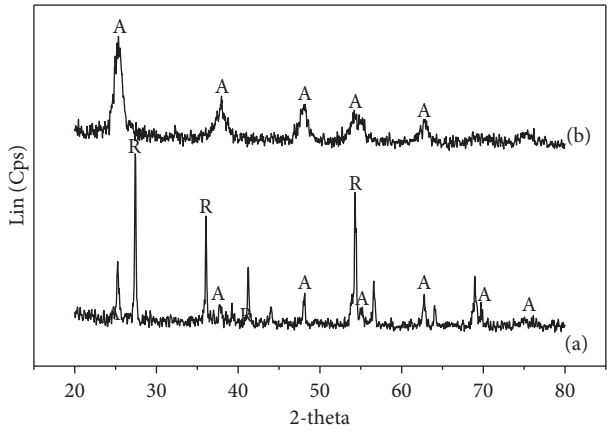

Figure 1: XRD patterns of TiO_2 (a) and C, N-TiO_2 (b).

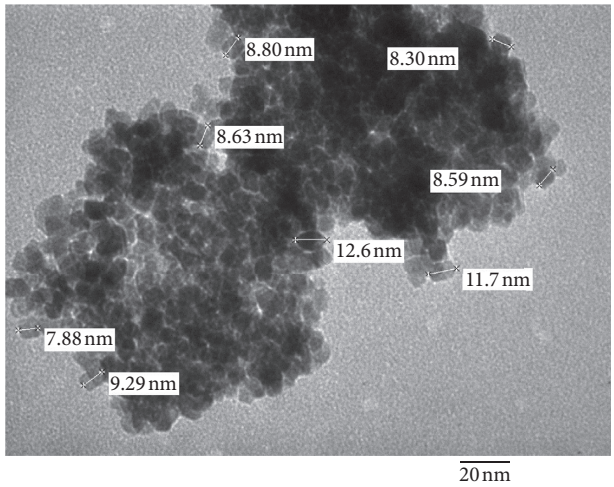

Figure 2: TEM image of C, N-TiO_2.

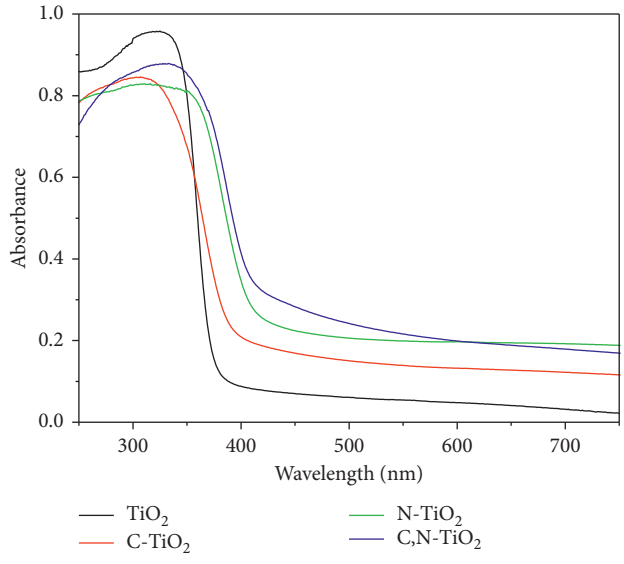

Figure 3: UV-VIS spectra of TiO_2 (a) and C, N-TiO_2 (b).

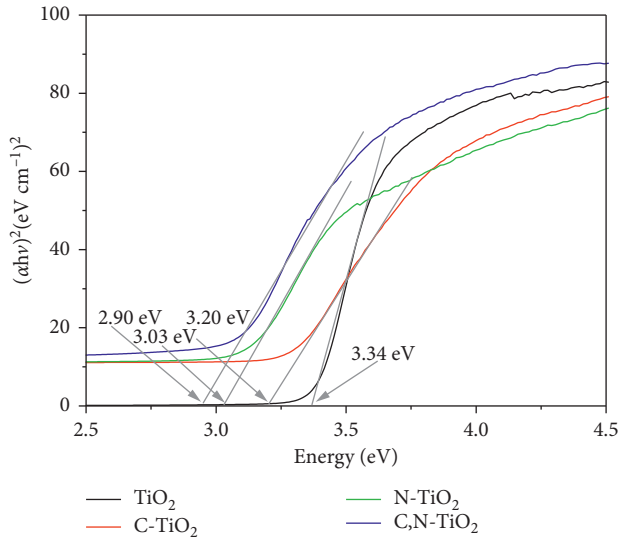

Figure 4: Plot of $[\alpha h\nu]^2$ vs h.ν for pristine TiO_2, C-TiO_2, N-TiO_2, and C,N-TiO_2.

absorption bands of C-TiO_2, N-TiO_2, and pristine TiO_2 (Figure 3).

The band gap energies estimated by using the Tauc method are 3.34, 3.20, 3.03, and 2.90 eV for pristine TiO_2, C-TiO_2, N-TiO_2, and C, N-TiO_2, respectively (Figure 4). The decrease in the energy band gap can be explained as follows: (i) when adding the carbon element, a part of carbon atoms will occupy the interstitial site in the crystal structure which is attributed to the decrease in the energy band gap [26]; (ii) N substitutes O, leading to a significant decrease in the energy band gap [3, 27]. Moreover, a part of carbon atoms cover on the surface of TiO_2 in the form of graphite or carbonate groups which would increase the photosentivity [3, 29]. The absorption edge shifts to the visible regions would be promising for the application of photocatalysts under sunlight irradiation.

The IR spectra showing a broad peak appearing at around 3450 cm^{-1} could be assigned to vibrations of hydroxyl groups on the surface of TiO_2 in the form of Ti-OH (Figure 5). In addition, the peak at 1647 cm^{-1} is likely due to vibrations of hydroxyl groups in the form of Ti-O-OH. The relatively weak peaks at 1540 cm^{-1} and around 1385 cm^{-1} could be attributed to the vibration of C=O and C-O in the carbonate group, respectively (Figure 5). The presence of those functional groups on the TiO_2 surface would lead to an increase in photosensitivity of the as-synthesized catalysts [26].

The presence of the N element in the catalyst obtained is approved by the peak at 1400 cm^{-1}, which is likely due to vibrations of N-H bonds. In addition, multiple bands at the region of 536–484 cm^{-1} are assigned to vibrations of Ti-O and Ti-O-C bonds. This is in agreement with the results of EDX analysis (Figure 6), which reveal the presence of Ti, O, C, and N elements in the samples. It is noted that the formation of bonds between C and N elements and TiO_2 could be examined by using the X-ray photoelectron spectroscopy (XPS) method [24, 25].

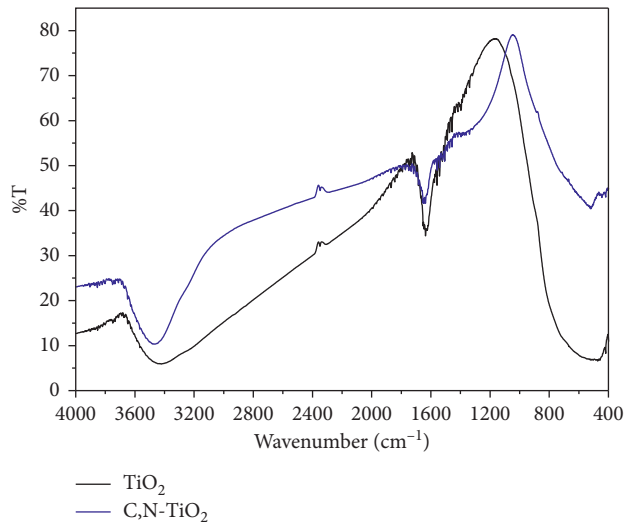

Figure 5: IR spectra of TiO_2 (a) and C, N-TiO_2 (b).

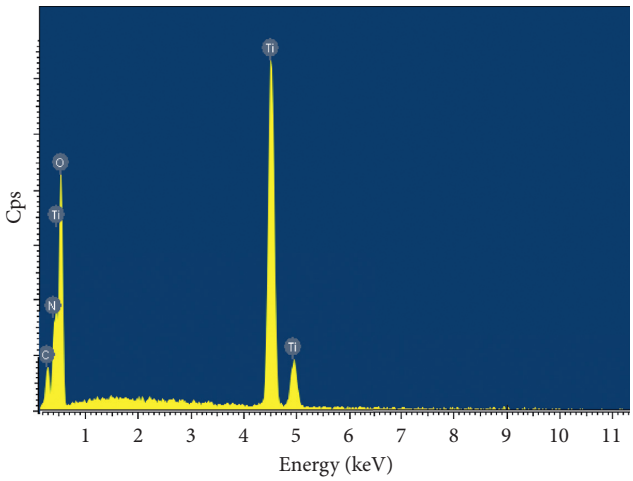

Figure 6: EDX analysis of C, N-TiO_2.

BET analysis was carried out under nitrogen atmosphere to figure out the porous features of the prepared synthesized materials, which is presented in Figure 7. The adsorption/desorption plots of C, N-TiO_2 show a common type IV isotherm with a H3 hysteresis loop. Furthermore, the BJH analysis shows a wide distribution of hierarchical pores with diameters in the range of meso-macro pores (Figure S2); the pore volume for C, N-TiO_2 is 0.040 cm^3/g.

It is noted that the BET specific surface area of the prepared C, N-TiO_2 is 20.3 m^2/g. This figure is slightly higher when compared to the values previously reported for pristine TiO_2. For instance, Hussain et al. [30] reported that TiO_2 commercial (anatase/technical) could present a BET specific surface area in the range of 10–15 m^2/g, while the increase in rutile percentage could lead to an augmentation of the surface area of TiO_2. Similarly, Shi et al. [31] revealed that anatase TiO_2 exhibited a BET surface area lower than 5 m^2/g, and the latter would decrease when the treatment temperature increases. Mahlambi et al. [32] synthesized

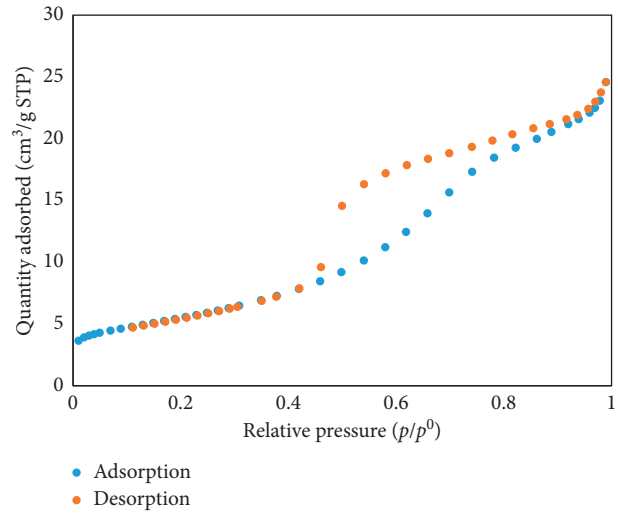

Figure 7: Nitrogen adsorption-desorption isotherms for the C, N-TiO_2 photocatalyst.

TiO_2 nanoparticles and found that at 550°C their specific surface areas were 22.72 m^2/g, and this value decreased to 7.78 m^2/g when the treatment temperature increased to 600°C.

3.2. Photocatalytic Performance of C, N-TiO_2 towards RhB Degradation. The results in Figure 8 indicate that the RhB degradation efficiency under visible-light condition of C, N-TiO_2 is higher than that of pure TiO_2. As for C, N-TiO_2, the degradation efficiency reached up to 94% after 90 min of irradiation. This is consistent with the characteristics of the obtained catalyst.

Studying the effect of the C, N-TiO_2 content on the RhB degradation efficiency (Figure 9) suggests that the optimal amount of the catalyst is 1.8 g/L. Using a large amount of catalyst caused the photoresist, resulting in a decrease in catalytic activity.

According to the results obtained from liquid UV-Vis measurements of the RhB solution by C, N-TiO_2 as a function of treatment time (Figure 10), RhB changed over time. As for the initial RhB solution of 920 mg/L, the characteristic peak at 533 nm moved to the peaks of the intermediate organic compounds. The peak intensity of these compounds decreases with increasing treatment time and is extremely low (near zero) after 3 hours of treatment. This suggests that the role of C, N-TiO_2 in the RhB degradation is different from the normal absorption processes [33, 34].

It should be noted that the RhB degradation efficiency is extremely low in the dark (Figure 11), indicating that the catalyst obtained is a photocatalyst. The RhB degradation efficiency under compact lamp and natural light irradiation is almost the same because of the 36 W compact lamp containing wavelength at 450 nm near absorption maximum of the catalyst. Hence, the obtained catalyst works well in visible light and natural light, and it is in agreement with previous reported works [35–37].

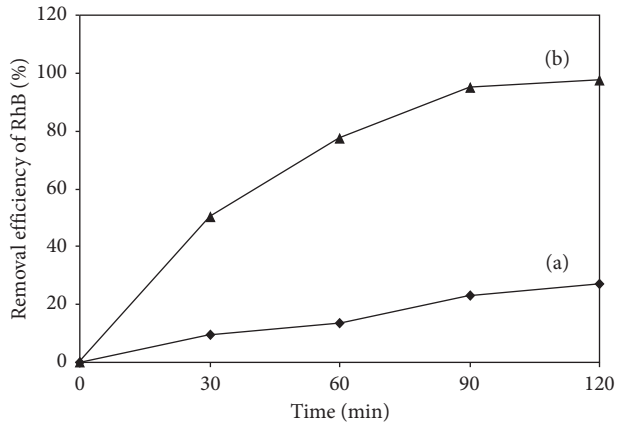

Figure 8: Comparison of degradation efficiency as a function of light irradiation time of TiO_2 (a) and C, N-TiO_2 (b).

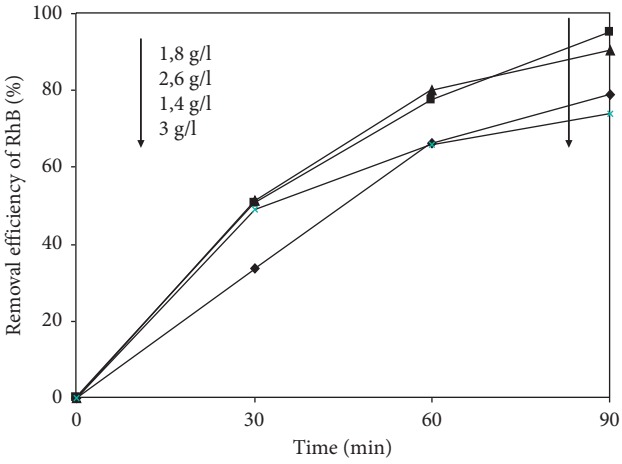

Figure 9: Effect of catalyst concentration on the RhB degradation efficiency of C, N-TiO_2.

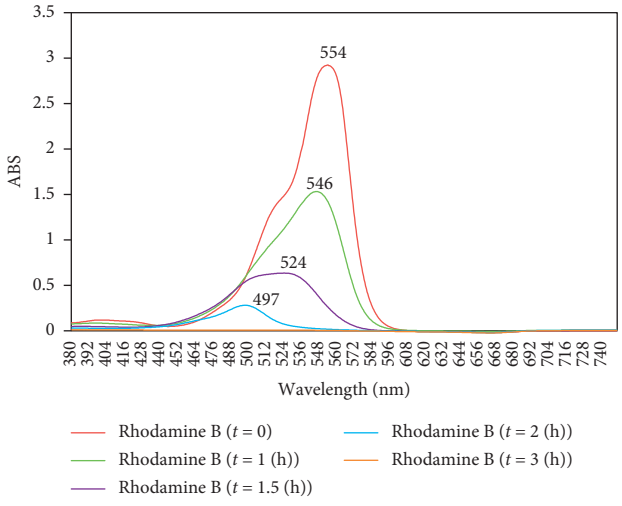

Figure 10: Liquid UV-Vis spectra of the RhB solution as a function of treatment time.

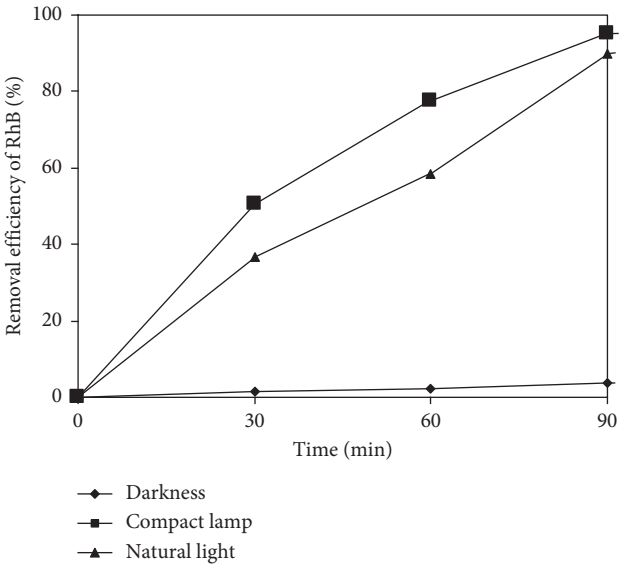

Figure 11: RhB degradation efficiency of C, N-TiO_2 under different irradiation conditions.

3.3. Kinetics of RhB Degradation by C, N-TiO_2 under Visible-Light Irradiation. Kinetics of the RhB degradation reaction was studied by using different initial concentrations of RhB (0–100 mg/L) while keeping the catalyst load constant at 1.8 g/L.

RhB decomposition reaction can be described by the Langmuir–Hinshelwood kinetics equation that is expressed as follows [27]:

$$r = -\frac{dC}{dt} = k\frac{KC}{1 + KC}, \tag{2}$$

where k is the reaction rate constant, K is the adsorption coefficient, t is the time, and C is the reactant concentration (the target organic compound). In the case of low initial concentrations, $KC << 1$, equation (2) can be rewritten as the following:

$$r = -\frac{dC}{dt} = k \cdot KC = k' \cdot C, \tag{3}$$

where k' is the apparent rate constant which is also known as the reduced first-order reaction. Then, the following equation is derived:

$$\ln \frac{C_o}{C_t} = k' \cdot t, \tag{4}$$

where C_o and C_t are the reactant concentrations at $t = 0$ and t (min), respectively. Figure 12 shows the dependence of $\ln C_o/C_t$ on time during the degradation of RhB by the C, N-TiO_2 photocatalyst.

As can be seen in Figures 12 and 13, when the initial concentrations of RhB were in the range of 0–100 mg/L, the photodegradation was divided into 3 distinct groups, which were characterized by the corresponding distinct apparent rate constants. The decomposition of RhB was observed unstable when the initial concentration was relatively low (0–10 mg/L). This is due to the degradation mainly affected by the absorption

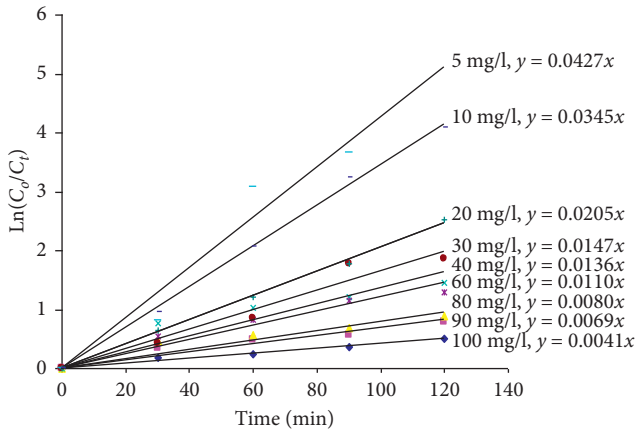

Figure 12: First-order kinetics for RhB degradation at different initial concentrations.

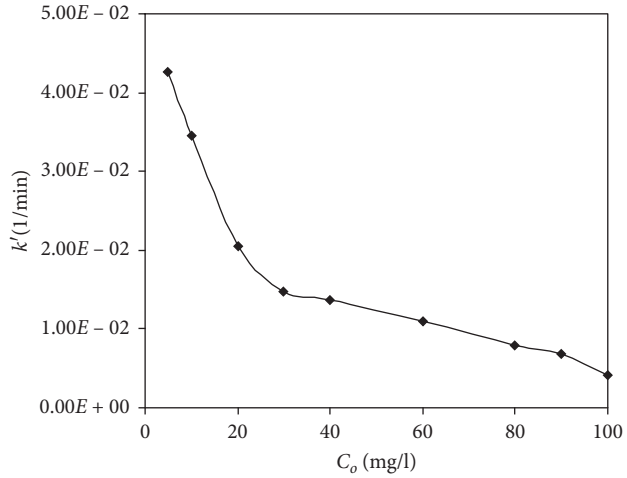

Figure 13: The apparent rate constant k' as a function of initial concentrations of RhB.

process. The corresponding apparent rate constant k' is 0.0427 min^{-1}. In contrast, when the initial concentration was relatively high (>10 mg/L), the RhB decomposition occurred very slowly, resulting in smaller apparent rate constants (k' = 0.0041 min^{-1} for 100 mg/L). This is because the bold color of RhB causes the photoresist [23, 27]. The suitable initial concentration for stable decomposition is about 20–40 mg/L. The optimal initial concentration of RhB is 20 mg/L at which the apparent rate constant k' is 0.0205 min^{-1}. The results obtained in this work is in agreement with previous studies [27, 32]. Hence, with the RhB initial concentration of 20 mg/L, equation (4) can be expressed by the following:

$$\ln \frac{C_o}{C_t} = 0.0205 \times t. \quad (5)$$

Similarly, the relation between C_o/C_t and t for other initial concentrations of RhB could be plotted as in Figure 13.

The photocatalytic degradation of RhB by the C, N-TiO_2 system can be explained by the following mechanism (Figure 14): (1) once $h\nu \geq (EC–EV')$, electrons would be excited in the valence band of TiO_2 by the process: $TiO_2 + h\nu$ (UV) $\longrightarrow$ TiO_2 ($e_{CB}^- + h_{VB}^+$); (2) the departed electrons and holes subsequently migrate to the surface of the catalysts and react with adsorbed H_2O and O_2 molecules, forming $^\bullet OH$ and $^\bullet O_2^-$, respectively, according to equations (6)–(8):

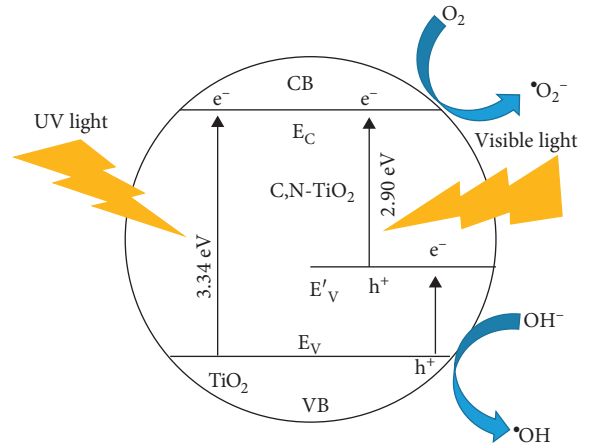

Figure 14: Schematic mechanism of photocatalytic degradation of RhB by C, N-TiO_2.

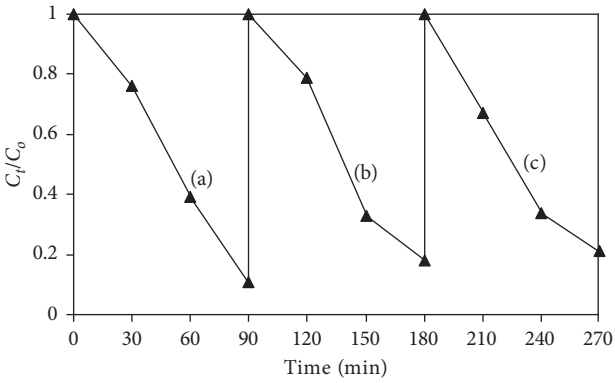

Figure 15: Catalyst's reuse results: (a) first cycle; (b) second cycle; (c) third cycle.

$$H_2O + h_{VB}^+ \longrightarrow {}^\bullet OH + H^+ \quad (6)$$

$$HO_{ad}^- + h_{VB}^+ \longrightarrow {}^\bullet OH_{ad} \quad (7)$$

$$e_{CB}^- + O_2 \longrightarrow {}^\bullet O_2^- \quad (8)$$

and (3) $^\bullet OH$ and $^\bullet O_2^-$ radicals are mainly responsible for the degradation of RhB in solutions [38]. The mechanism for the degradation of RhB in solutions by the C, N-TiO_2 system is proposed in Figure 14.

3.4. Recoverability and Reusability of C, N-TiO_2 Photocatalyst. The catalytic stability in RhB decomposition under visible-light irradiation was studied. After each decomposition cycle, the catalyst was centrifuged, washed with distilled water, and then used for further treatment of RhB in solutions. As can be seen in Figure 15, C and N codoped TiO_2 exhibited good catalytic

activity with the degradation efficiency of above 86% after three cycles, and the obtained results were in agreement with previous studies [39]. It is noted that the absence of RhB and other substances on the surface of the catalyst and no release of catalysts to the water medium need to be proved prior to each subsequent cycle. This could be revealed by using TEM, FT-IR, BET, and extinction spectrum change of the water solution [22]. In this work, the photocatalytic performance is still very high after three cycles (86%), suggesting that the presence of substances on the catalyst's surfaces is insignificant.

4. Conclusions

In this work, C and N codoped TiO_2 nanoparticles are successfully prepared by solvothermal synthesis and then used for the study on their catalytic activities regarding RhB degradation in solutions under visible-light irradiation. The obtained results showed that the as-synthesized nanoparticles mainly contained anatase crystallites, with an average particle diameter of 9.1 nm. C, N-TiO_2 presented a high catalytic activity in the RhB degradation under visible-light irradiation. The optimal catalyst dosage was 1.8 g/L, while optimal initial concentration of RhB was 5 mg/L. The photocatalytic degradation kinetics was found to follow the first-order rate law of the Langmuir–Hinshelwood model. The apparent rate constant depended on the initial concentration of RhB, which was higher at more diluted solutions of RhB.

Data Availability

All the data used to support the findings of this study are provided within the manuscript.

Conflicts of Interest

The authors declare that there are no conflicts of interest regarding the publication of this paper.

Acknowledgments

This work was partly supported by the Team Project of VLIR-UOS with the code number ZEIN2016PR431. The authors would like to thank the OEPAC project for the utilization of instruments.

Supplementary Materials

Figure S1: energy spectra of the deployed compact lamp. Figure S2: BJH adsorption analysis for the C, N-TiO_2 photocatalyst. (*Supplementary Materials*)

References

[1] H. Liu, Y. Wu, and J. Zhang, "A new approach toward carbon-modified vanadium-doped titanium dioxide photocatalysts," *ACS Applied Materials & Interfaces*, vol. 3, no. 5, pp. 1757–1764, 2011.

[2] S. Jafari, B. Tryba, E. Kusiak-Nejman, J. Kapica-Kozar, A. W. Morawski, and M. Sillanpää, "The role of adsorption in the photocatalytic decomposition of Orange II on carbon-modified TiO_2," *Journal of Molecular Liquids*, vol. 220, pp. 504–512, 2016.

[3] Y. Taga, "Titanium oxide based visible light photocatalysts: materials design and applications," *Thin Solid Films*, vol. 517, no. 10, pp. 3167–3172, 2009.

[4] S. Hosseini, H. Jahangirian, T. J. Webster, S. M. Soltani, and M. K. Aroua, "Synthesis, characterization, and performance evaluation of multilayered photoanodes by introducing mesoporous carbon and TiO_2 for humic acid adsorption," *International Journal of Nanomedicine*, vol. 11, pp. 3969–3978, 2016.

[5] G. Zhang, Y. C. Zhang, M. Nadagouda et al., "Visible light-sensitized S, N and C co-doped polymorphic TiO_2 for photocatalytic destruction of microcystin-LR," *Applied Catalysis B: Environmental*, vol. 144, pp. 614–621, 2014.

[6] S. D. Richardson, C. S. Willson, and K. A. Rusch, "Use of rhodamine water tracer in the marshland upwelling system," *Ground Water*, vol. 42, no. 5, pp. 678–688, 2004.

[7] D. J. Dire and J. A. Wilkinson, "Acute exposure to rhodamine B," *Journal of Toxicology: Clinical Toxicology*, vol. 25, no. 7, pp. 603–607, 1987.

[8] D. Kornbrust and T. Barfknecht, "Testing of 24 food, drug, cosmetic, and fabric dyes in the in vitro and the in vivo/in vitro rat hepatocyte primary culture DNA repair assays," *Environmental Mutagenesis*, vol. 7, no. 1, pp. 101–120, 1985.

[9] E. R. Nestmann, G. R. Douglas, T. I. Matula, C. E. Grant, and D. J. Kowbel, "Mutagenic activity of rhodamine dyes and their impurities as detected by mutation induction in Salmonella and DMA damage in Chinese hamster ovary cells," *Cancer Research*, vol. 39, pp. 4412–4417, 1979.

[10] S. Zodi, B. Merzouk, O. Potier, F. Lapicque, and J.-P. Leclerc, "Direct red 81 dye removal by a continuous flow electrocoagulation/flotation reactor," *Separation and Purification Technology*, vol. 108, pp. 215–222, 2013.

[11] Y.-M. Zheng, R. F. Yunus, K. G. N. Nanayakkara, and J. P. Chen, "Electrochemical decoloration of synthetic wastewater containing rhodamine 6G: behaviors and mechanism," *Industrial & Engineering Chemistry Research*, vol. 51, no. 17, pp. 5953–5960, 2012.

[12] H. K. Shon, S. Vigneswaran, I. S. Kim et al., "Preparation of titanium dioxide (TiO_2) from sludge produced by titanium tetrachloride (TiCl4) flocculation of wastewater," *Environmental Science & Technology*, vol. 41, no. 4, pp. 1372–1377, 2007.

[13] X. Chen, Z. Xue, Y. Yao, W. Wang, F. Zhu, and C. Hong, "Oxidation degradation of rhodamine B in aqueous by UV/S2O82- treatment system," *International Journal of Photoenergy*, vol. 2012, Article ID 754691, 9 pages, 2012.

[14] W. Griffith, "Ozonolysis in coordination chemistry and catalysis: recent advances," *Coordination Chemistry Reviews*, vol. 219–221, pp. 259–281, 2001.

[15] K. Shen and M. A. Gondal, "Removal of hazardous Rhodamine dye from water by adsorption onto exhausted coffee ground," *Journal of Saudi Chemical Society*, vol. 21, pp. S120–S127, 2017.

[16] T. A. Khan, M. Nazir, and E. A. Khan, "Adsorptive removal of rhodamine B from textile wastewater using water chestnut (*Trapa natans* L.) peel: adsorption dynamics and kinetic studies," *Toxicological & Environmental Chemistry*, vol. 95, no. 6, pp. 919–931, 2013.

[17] A. A. Oyekanmi, A. Ahmad, K. Hossain, and M. Rafatullah, "Adsorption of Rhodamine B dye from aqueous solution onto acid treated banana peel: response surface methodology, kinetics and isotherm studies," *PLoS ONE*, vol. 14, no. 5, Article ID e0216878, 2019.

[18] S. Elumalai and G. Muthuraman, "Comparative study of liquid–liquid extraction and bulk liquid membrane for rhodamine B," *International Journal of Engineering and Innovative Technology*, vol. 3, no. 2, pp. 387–392, 2013.

[19] M. E. Ersahin, H. Ozgun, R. K. Dereli, I. Ozturk, K. Roest, and J. B. van Lier, "A review on dynamic membrane filtration: materials, applications and future perspectives," *Bioresource Technology*, vol. 122, pp. 196–206, 2012.

[20] A. Phuruangrat, A. Maneechote, P. Dumrongrojthanath, N. Ekthammathat, S. Thongtem, and T. Thongtem, "Effect of pH on visible-light-driven Bi2WO6 nanostructured catalyst synthesized by hydrothermal method," *Superlattices and Microstructures*, vol. 78, pp. 106–115, 2015.

[21] P. Dumrongrojthanath, T. Thongtem, A. Phuruangrat, and S. Thongtem, "Synthesis and characterization of hierarchical multilayered flower-like assemblies of Ag doped Bi2WO6 and their photocatalytic activities," *Superlattices and Microstructures*, vol. 64, pp. 196–203, 2013.

[22] S. Y. Lee, D. Kang, S. Jeong, H. T. Do, and J. H. Kim, "Photocatalytic degradation of rhodamine B dye by TiO_2 and gold nanoparticles supported on a floating porous polydimethylsiloxane sponge under ultraviolet and visible light irradiation," *ACS Omega*, vol. 5, no. 8, pp. 4233–4241, 2020.

[23] T. T. T. Le, T. L. Nguyen, D. T. Tran, and V. N. Nguyen, "Enhanced photocatalytic degradation of rhodamine B using C/Fe Co-doped titanium dioxide coated on activated carbon," *Journal of Chemistry*, vol. 2019, Article ID 2949316, 8 pages, 2019.

[24] J. Shao, W. Sheng, M. Wang et al., "In situ synthesis of carbon-doped TiO 2 single-crystal nanorods with a remarkably photocatalytic efficiency," *Applied Catalysis B: Environmental*, vol. 209, pp. 311–319, 2017.

[25] Y. Zhang, J. Chen, L. Hua et al., "High photocatalytic activity of hierarchical SiO2@C-doped TiO_2 hollow spheres in UV and visible light towards degradation of rhodamine B," *Journal of Hazardous Materials*, vol. 340, pp. 309–318, 2017.

[26] C. Chen, M. Long, H. Zeng et al., "Preparation, characterization and visible-light activity of carbon modified TiO_2 with two kinds of carbonaceous species," *Journal of Molecular Catalysis A: Chemical*, vol. 314, no. 1-2, pp. 35–41, 2009.

[27] W. Xiaoping and T.-T. Lim, "Solvothermal synthesis of C-N codoped TiO_2 and photocatalytic evaluation for bisphenol A degradation using a visible-light irradiation LED photoreactor," *Applied Catalysis B: Environmental*, vol. 100, pp. 355–364, 2010.

[28] U. G. Akpan and B. H. Hameed, "The advancements in sol-gel method of doped-TiO_2 photocatalysts," *Applied Catalysis A: General*, vol. 375, no. 1, pp. 1–11, 2010.

[29] H. J. Yun, H. Lee, J. B. Joo, N. D. Kim, M. Y. Kang, and J. Yi, "Facile preparation of high performance visible light sensitive photo-catalysts," *Applied Catalysis B: Environmental*, vol. 94, no. 3-4, pp. 241–247, 2010.

[30] M. Hussain, R. Ceccarelli, D. L. Marchisio, D. Fino, N. Russo, and F. Geobaldo, "Synthesis, characterization, and photocatalytic application of novel TiO_2 nanoparticles," *Chemical Engineering Journal*, vol. 157, no. 1, pp. 45–51, 2010.

[31] T. Shi, Y. Duan, K. Lv et al., "Photocatalytic oxidation of acetone over high thermally stable TiO_2 nanosheets with exposed (001) facets," *Frontiers in Chemistry*, vol. 6, p. 175, 2018.

[32] M. M. Mahlambi, A. K. Mishra, S. B. Mishra, R. W. Krause, B. B. Mamba, and A. M. Raichur, "Comparison of rhodamine B degradation under UV irradiation by two phases of titania nano-photocatalyst," *Journal of Thermal Analysis and Calorimetry*, vol. 110, no. 2, pp. 847–855, 2012.

[33] W. Zhang, Y. Li, C. Wang, and P. Wang, "Kinetics of heterogeneous photocatalytic degradation of Rhodamine B by TiO_2-coated activated carbon: roles of TiO_2 content and light intensity," *Desalination*, vol. 266, no. 1-3, pp. 40–45, 2011.

[34] Y. Xiao, X. Sun, l. Li et al., "Simultaneous formation of a C/N-TiO_2 hollow photocatalyst with efficient photocatalytic performance and recyclability," *Chinese Journal of Catalysis*, vol. 40, no. 5, pp. 765–775, 2019.

[35] Y. Wu, J. Zhang, L. Xiao, and F. Chen, "Properties of carbon and iron modified TiO_2 photocatalyst synthesized at low temperature and photodegradation of acid orange 7 under visible light," *Applied Surface Science*, vol. 256, no. 13, pp. 4260–4268, 2010.

[36] X. Cheng, X. Yu, and Z. Xing, "Synthesis and characterization of C-N-S-tridoped TiO_2 nano-crystalline photocatalyst and its photocatalytic activity for degradation of rhodamine B," *Journal of Physics and Chemistry of Solids*, vol. 74, no. 5, pp. 684–690, 2013.

[37] H. Huang, Y. Song, N. Li et al., "One-step in-situ preparation of N-doped TiO_2@C derived from Ti3C2 MXene for enhanced visible-light driven photodegradation," *Applied Catalysis B: Environmental*, vol. 251, pp. 154–161, 2019.

[38] L. Youji, Z. Xiaoming, C. Wei et al., "Photodecolorization of Rhodamine B on tungsten-doped TiO_2/activated carbon under visible-light irradiation," *Journal of Hazardous Materials*, vol. 227-228, pp. 25–33, 2012.

[39] A. Y. Shan, T. I. M. Ghazi, and S. A. Rashid, "Immobilisation of titanium dioxide onto supporting materials in heterogeneous photocatalysis: a review," *Applied Catalysis A: General*, vol. 389, no. 1-2, pp. 1–8, 2010.